Technical Note on CERES EBAF-Surface Ed2.6r

Surface Downwelling Longwave Radiation (rlds)
Surface Upwelling Longwave Radiation (rlus)
Surface Downwelling Shortwave Radiation (rsds)
Surface Upwelling Shortwave Radiation (rsus)
Surface Downwelling Clear-Sky Shortwave Radiation (rsdscs)
Surface Upwelling Clear-Sky Shortwave Radiation (rsuscs)
Surface Downwelling Clear-Sky Longwave Radiation (rldscs)

1. Intent of This Document and Point of Contact (POC)

1a) This document is intended for users who wish to compare satellite-based estimate of surface radiative fluxes (irradiances) with climate model output in the context of the CMIP5/IPCC historical experiments. This document describes essential information about surface irradiances for this dataset needed for the comparison. References that provide more detailed information are provided at the end of this document.

This NASA dataset is provided as part of an experimental activity to increase the usability of NASA satellite observational data for the modeling and model analysis communities. This is not a standard NASA satellite instrument product, but does represent an effort on behalf of data experts to identify a product that is appropriate for routine model evaluation. The data may have been reprocessed, reformed, or created solely for comparisons with climate model output. Community feedback to improve and validate the dataset for modeling usage is appreciated. Email comments to
HQ-CLIMATE-OBS@mail.nasa.gov.

Dataset File Name (as it appears on the ESG):

rlds_CERES-EBAF_L4_Ed2-6r_200003-201002.nc
rlus_CERES-EBAF_L4_Ed2-6r_200003-201002.nc
rsds_CERES-EBAF_L4_Ed2-6r_200003-201002.nc
rsus_CERES-EBAF_L4_Ed2-6r_200003-201002.nc
rsdscs_CERES-EBAF_L4_Ed2-6r_200003-201002.nc
rsuscs_CERES-EBAF_L4_Ed2-6r_200003-201002.nc
rldscs_CERES-EBAF_L4_Ed2-6r_200003-201002.nc

1b) Technical point of contact for this dataset:

Seiji Kato email: Seiji.Kato@nasa.gov

2. Data Field Description

CF variable name, units:	Surface Downwelling Longwave Radiation (rlds) Wm^{-2} Surface Upwelling Longwave Radiation (rlus) Wm^{-2} Surface Downwelling Shortwave Radiation (rsds) Wm^{-2} Surface Upwelling Shortwave Radiation (rsus) Wm^{-2} Surface Downwelling Clear-Sky Shortwave Radiation (rsdscs) Wm^{-2} Surface Upwelling Clear-Sky Shortwave Radiation (rsuscs) Wm^{-2} Surface Downwelling Clear-Sky Longwave Radiation (rldscs) Wm^{-2}
Spatial resolution:	1°×1° latitude by longitude
Temporal resolution and extent:	Monthly averaged from 03/2000 to 02/2010
Coverage	Global

3. Data Origin

Surface irradiances included in this dataset are from CERES Energy Balanced and Filled (EBAF)-Surface Ed2.6r data product (Kato et al. 2012a). They are computed using MODIS-derived cloud properties (Minnis et al. 2011) and atmospheric properties (temperature and humidity profiles) given by the Goddard Earth Observing System (GEOS-4 and 5) Data Assimilation System reanalysis (Bloom et al. 2005; Rienecker et al. 2008). To account for the diurnal cycle of cloud properties between 60°N and 60°S latitude, cloud fraction and cloud top height derived from five geostationary satellites (Minnis et al. 1994) are also used. Geostationary satellites are calibrated against MODIS (Doelling et al. 2012). Other inputs for irradiance computations include ozone amount (Yang et al. 2000), ocean spectral surface albedo from Jin et al. (2004), and broadband land surface albedos that are inferred from the clear-sky CERES measurements (Rutan et al. 2009). Because computed TOA irradiances do not necessarily agree with CERES-derived TOA irradiances, computed TOA irradiances are adjusted to be consistent with CERES-derived TOA outgoing shortwave radiation (rsut, rsutcs for clear-sky) and outgoing longwave radiation (rlut, rlutcs for clear-sky) from EBAF-TOA Ed2.6r (Loeb et al. 2009; Loeb et al. 2012). TOA irradiance adjustments are made by adjusting inputs (surface, atmospheric, and cloud properties). In the adjustment process, CALIPSO, CloudSat, and AIRS observations are used to constrain cloud and atmospheric properties (Kato et al. 2012a).

4. Validation and Uncertainty Estimate

Regional monthly mean downward shortwave and longwave irradiances are compared with surface observations. A comparison of 10 years of coincident satellite-derived and surface-observed monthly mean irradiances for a number of sites shows that the bias (RMS difference) is 4.7 (13.3) Wm^{-2} for downward shortwave and -2.5 (7.1) Wm^{-2} for downward longwave over ocean and -1.7 (7.8) Wm^{-2} for downward shortwave and -1.0 (7.6) Wm^{-2} for downward longwave irradiances over land (Kato et al. 2012a).

The estimated uncertainty in 1°×1° regional surface irradiances (Kato et al. 2012b) is given in Table 1.

Table 1: Summary of uncertainties in the monthly 1°×1° gridded irradiance computed with satellite-derived cloud and aerosol properties in Wm^{-2} (after Kato et al. 2012b).

		Mean value	Estimated uncertainty
Downward longwave	Ocean+land[1]	345	14
	Ocean	354	12
	Land	329	17
Upward longwave	Ocean+Land[1]	398	15
	Ocean	402	13
	Land	394	19
Downward shortwave	Ocean+Land[1]	192	10
	Ocean	190	9
	Land	203	12
Upward shortwave[2]	Ocean+Land[1]	23	11
	Ocean	12	11
	Land	53	12

[1] Mean of ocean and land uncertainties
[2] Excludes polar regions where detecting sea ice or snow gives a large uncertainty in the upward shortwave irradiance.

5. Consideration for Model-Observation Comparisons

As mentioned earlier, clear-sky surface irradiances are constrained by CERES observations. As a result, the computed clear-sky irradiances are averaged by weighting by the clear-sky fraction. In contrast, climate models compute clear-sky irradiance by removing clouds. These two methods can produce significant differences in computed clear-sky irradiances. The clear-sky fraction-weighted surface downward longwave irradiance tends to be smaller than clear-sky surface downward longwave irradiance computed by removing clouds because observed clear-sky conditions happen when atmospheres tend to be dryer (Sohn et al. 2010). Figures 1 and 2 show the difference of clear-sky irradiances computed with clouds removed and using clear-sky fraction weighting.

Other cautions in using this dataset for comparisons include:

- The source of temperature and humidity profiles for surface flux calculations changes from GEOS-4 to GEOS-5 starting in November 2007. When deseasonalized anomalies are calculated separately for land and ocean, the time series of deseasonalized surface fluxes shows a discontinuity between October 2007 and November 2007.
- The near-surface temperature is significantly larger and near-surface water vapor amount is also significantly larger in GEOS-4 over the tropics in 2004 compared to those in GEOS-5. We believe that GEOS-5 temperature and water vapor amount are more realistic because they are in accord with surface skin temperature anomalies. Because GEOS-4 is used before November 2007, the temperature and water vapor amount errors contribute to increasing deseasonalized anomalies of the downward longwave irradiance in 2004 when 10-year means are used to compute the anomalies. A reprocessing effort is currently underway.

- Clear-sky net shortwave irradiance is sometimes negative in polar regions (north of 60°N and south of 60°S). In other words, the upward shortwave irradiance is greater than downward shortwave irradiance. This is frequently caused by the constraint to the TOA irradiance near the terminator where twilight flux (Kato and Loeb 2003) has been added to reflected shortwave irradiance for EBAF-TOA. Note that the negative clear-sky net shortwave irradiance also affects the cloud effect of the net shortwave surface irradiance.

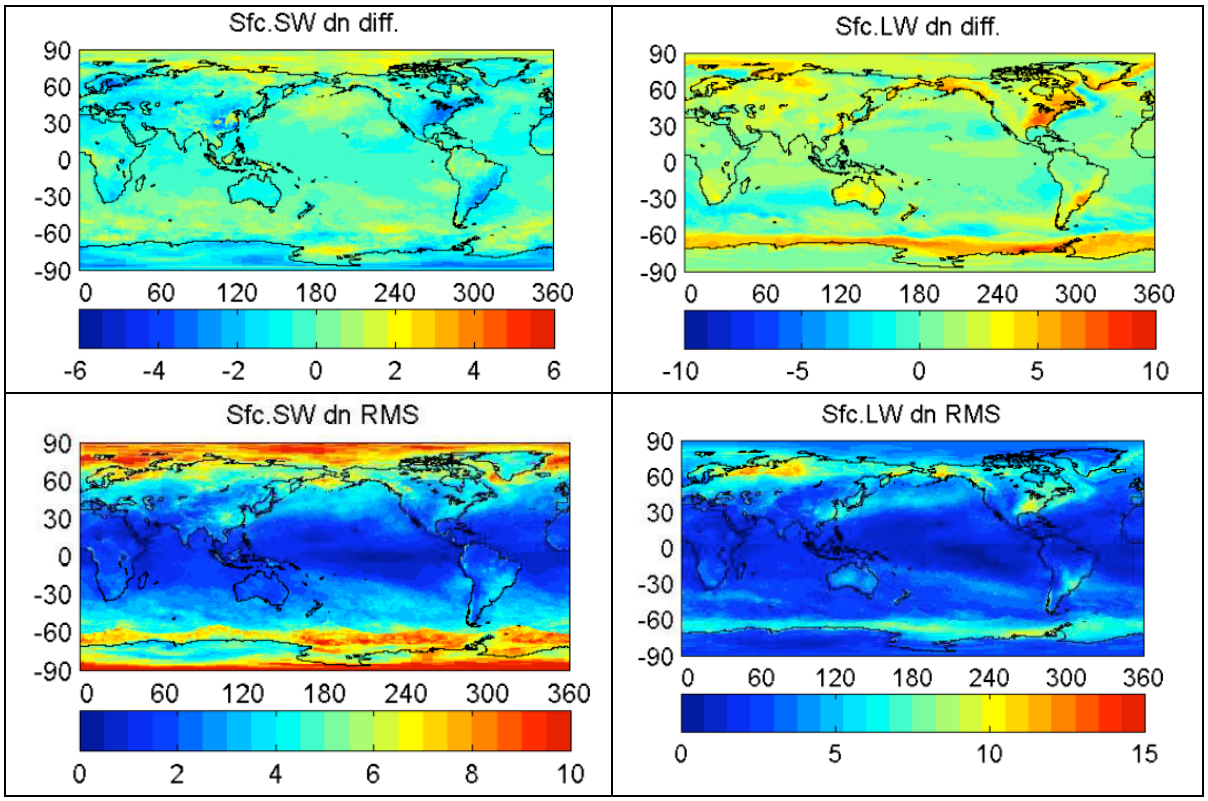

Figure 1. (Top) Difference, defined as clear-sky irradiances computed with clouds removed minus clear-sky fraction-weighted irradiances, of clear-sky surface downward shortwave (left) and downward longwave (right) irradiances in W m^{-2}. Differences are computed using 10 years of monthly 1°×1° gridded mean irradiances from March 2000 through February 2010. (Bottom) RMS difference of cloud-removed and clear-sky fraction-weighted surface downward shortwave irradiances (left) and surface downward longwave irradiances (right) in W m^{-2}, also computed using 10 years of monthly 1°×1° gridded mean irradiances.

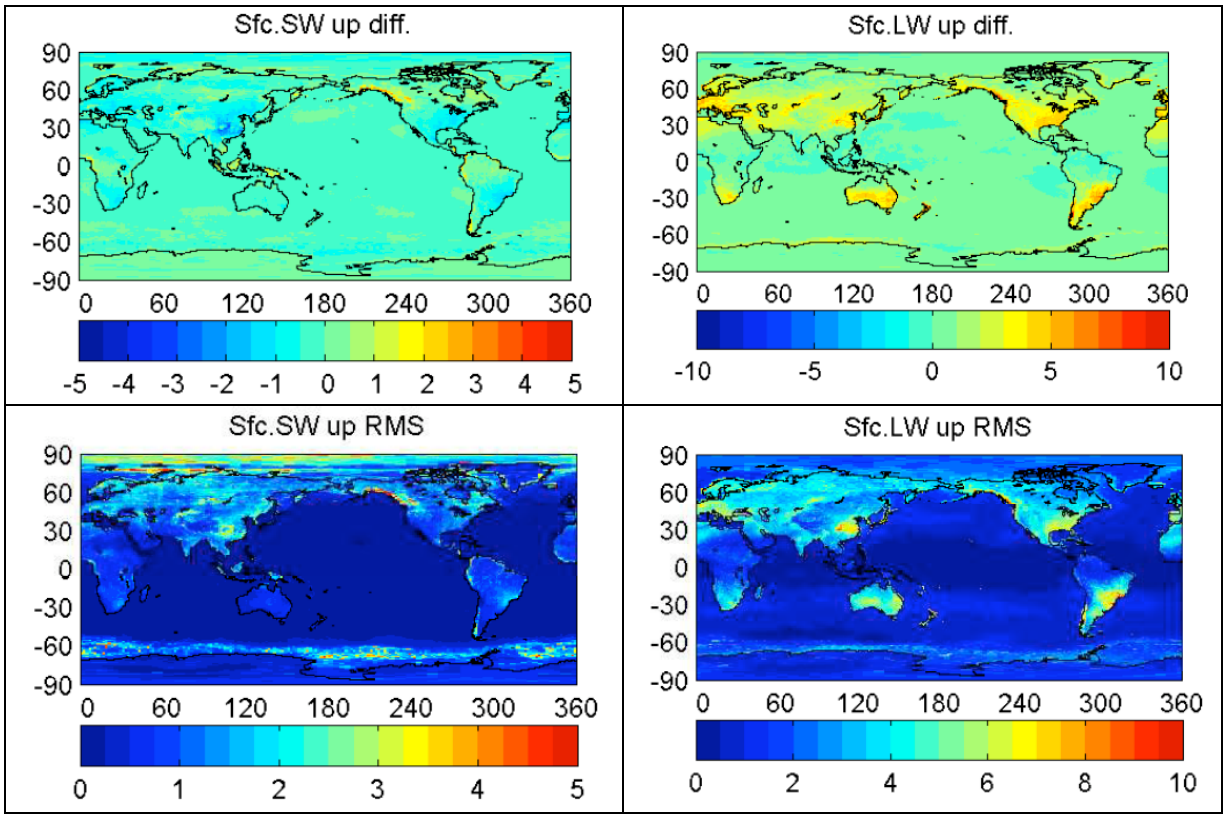

Figure 2. (Top) Difference, defined as clear-sky irradiances computed with clouds removed minus clear-sky fraction-weighted irradiances, of clear-sky surface upward shortwave (left) and upward longwave (right) irradiances in W m^{-2}. Differences are computed using 10 years of monthly 1°×1° gridded mean fluxes from March 2000 through February 2010. (Bottom) RMS difference of cloud-removed and clear-sky fraction-weighted surface upward shortwave irradiances (left) and surface upward longwave irradiances (right) in W m^{-2}, also computed using 10 years of monthly 1°×1° gridded mean irradiances.

6. CERES Instrument and Level 3 Products Overview

CERES instruments fly on the Terra (descending sun-synchronous orbit with an equator crossing time of 10:30 A.M. local time) and Aqua (ascending sun-synchronous orbit with an equator crossing time of 1:30 P.M. local time) satellites. Each CERES instrument measures filtered radiances in the shortwave (SW; wavelengths between 0.3 and 5 μm), total (TOT; wavelengths between 0.3 and 200 μm), and window (WN; wavelengths between 8 and 12 μm) regions. To correct for the imperfect spectral response of the instrument, the filtered radiances are converted to unfiltered reflected solar, unfiltered emitted terrestrial longwave (LW) and window (WN) radiances (Loeb et al. 2001). Since there is no LW channel on CERES, LW daytime radiances are determined from the difference between the TOT and SW channel radiances. Instantaneous top-of-atmosphere (TOA) irradiances are estimated from unfiltered radiances using empirical angular distribution models (ADMs; Loeb et al. 2003, 2005) for scene types identified using

retrievals from Moderate Resolution Imaging Spectrometer (MODIS) measurements (Minnis et al. 2011). Monthly mean irradiances are determined by spatially averaging the instantaneous values on a 1°×1° grid, temporally interpolating at 1-h increments for each hour of every month, and then averaging all hour boxes in a month. Level-3 processing is performed on a nested grid, which uses 1° equal-angle regions between 45°N and 45°S, and maintains area consistency at higher latitudes. The irradiances are then output to a complete 360x180 1°×1° grid created by replication.

7. References

The full version of CERES EBAF-Surface Ed2.6r is available from the following ordering site: http://ceres.larc.nasa.gov/order_data.php

Bloom, S. A., and coauthors, 2005: Documentation and validation of the Goddard Earth Observing System (GEOS) data assimilation system version-4, NASA Tech. Rep. NASA/TM-2005-104606, Vol. 26, 187 pp.

Doelling, D. R., N Loeb, D. F. Keyes, M. L. Nordeen, D. Morstad, B. A. Wielicki, D. F. Young, and M. Sun, 2012: Geostationary enhanced temporal interpolation for CERES flux products, submitted to *J. Atmos. Oceanic Technol*.

Jin, Z., T. P. Charlock, W. L. Smith, Jr., and K. Rutledge, 2004: A look-up table for ocean surface albedo. *Geophys. Res. Lett.,* **31**, L22301.

Kato, S. and N. G. Loeb, 2003: Twilight irradiance reflected by the Earth estimated from Clouds and the Earth's Radiant Energy System (CERES) measurements. *J. Climate*, 16, 2646-2650.

Kato, S., N. G. Loeb, F. G. Rose, D. R. Doelling, D. A. Rutan, T. E. Caldwell, L. Yu, and R. A. Weller, 2012a: Surface irradiances consistent with CERES-derived top-of-atmosphere shortwave and longwave irradiances, submitted to *J. Climate*.

Kato, S., N. G. Loeb, D. A. Rutan, F. G. Rose, S. Sun-Mack, W. F. Miller, and Y. Chen, 2012b: Uncertainty estimate of surface irradiances computed with MODIS-, CALIPSO-, and CloudSat-derived cloud and aerosol properties, *Surv. Geophys*., doi 10.1007/s10712-012-9179-x.

Loeb, N. G., K. J. Priestley, D. P. Kratz, E. B. Geier, R. N. Green, B. A. Wielicki, P. O. R. Hinton, and S. K. Nolan, 2001: Determination of unfiltered radiances from the Clouds and the Earth's Radiant Energy System (CERES) instrument. *J. Appl. Meteor*., 40, 822–835.

Loeb, N.G., N. M. Smith, S. Kato, W. F. Miller, S. K. Gupta, P. Minnis, and B. A. Wielicki, 2003: Angular distribution models for top-of-atmosphere radiative flux estimation from the Clouds and the Earth's Radiant Energy System instrument on the Tropical Rainfall Measuring Mission Satellite. Part I: Methodology. *J. Appl. Meteor*., 42, 240–265.

Loeb, N.G., S. Kato, K. Loukachine, and N. M. Smith, 2005: Angular distribution models for top-of-atmosphere radiative flux estimation from the Clouds and the Earth's Radiant Energy System instrument on the Terra satellite. Part I: Methodology. *J. Atmos. Oceanic Technol*., 22, 338–351.

Loeb, N. G., B. A. Wielicki, D. R. Doelling, G. L. Smith, D. F. Keyes, S. Kato, N. Manalo-Smith, and T. Wong, 2009: Toward optimal closure of the Earth's top-of-atmosphere radiation budget, *J. Climate*, 22, 748-766.

Loeb, N. G., J. M. Lyman, G. C. Johnson, R. P. Allan, D. R. Doelling, T. Wong, B. J. Soden, and G. L. Stephens, 2012: Observed changes in top-of-the-atmosphere radiation and upper-ocean heating consistent within uncertainty. *Nat. Geosci.*, 5, 110-113, doi:10.1038/NGEO1375.

Minnis, P. and coauthors, 2011: CERES Edition-2 cloud property retrievals using TRMM VIRS and Terra and Aqua MODIS data, Part I: Algorithms. *IEEE Trans. Geosci. Remote Sens.* 49, doi: 10.1109/TGRS.2011.2144601.

Minnis, P., W. L. Smith, Jr., D. P. Garber, J. K. Ayers, and D. R. Doelling, 1995: Cloud properties derived from GOES-7 for Spring 1994 ARM intensive observing period using Version 1.0.0 of ARM Satellite Data Analysis Program. NASA Ref. Pub. NASA-RP-1366, 62 pp.

Rienecker, M. M. and coauthors, 2008: The GEOS-5 Data Assimilation System-Documentation of Versions 5.0.1, 5.1.0, and 5.2.0. NASA Technical Report Series on Global Modeling and Data Assimilation, M. Suarez, Ed., NASA/TM-2008-104606, Vol. 27, 118 pp.

Rutan, D., F. Rose, M. Roman, N. Manalo-Smith, C. Schaaf, and T. Charlock, 2009: Development and assessment of broadband surface albedo from Clouds and the Earth's Radiant Energy System clouds and radiation swath data product, *J. Geophys. Res*., 114, D08125, doi:10.1029/2008JD010669.

Sohn, B. J., T. Nakajima, M. Satoh, and H.-S. Jang, 2010: Impact of different definitions of clear-sky flux on the determination of longwave cloud radiative forsing: NICAM simulation results, *Atmos. Chem. Phys*. 10, 11641-11646, doi:105194/acp-10-11641-2010.

Yang, S.-K., S. Zhou, and A. J. Miller, 2000: SMOBA: A 3-D daily ozone analysis using SBUV/2 and TOVS measurements, http://www.cpc.ncep.noaa.gov/products/stratosphere/SMOBA/smoba_doc.shtml.

8. Revision History

[Document changes in the dataset and the technical note if a new version replaces an older version published on the ESG.]

Rev 0 – 09/14/2012 – This is a new document/dataset.